Eur. Phys. J. B (2012) 85: 108
DOI: 10.1140/epjb/e2012-20820-1

THE EUROPEAN PHYSICAL JOURNAL B

Regular Article

A cluster theory for a Janus fluid

R. Fantoni[a]

National Institute for Theoretical Physics (NIThePP) and Institute of Theoretical Physics, Stellenbosch University, 7600 Stellenbosch, South Africa

Received 7 October 2011 / Received in final form 18 December 2011
Published online 28 March 2012 –

Abstract. Recent Monte Carlo simulations on the Kern and Frenkel model of a Janus fluid have revealed that in the vapour phase there is the formation of preferred clusters made up of a well-defined number of particles: the micelles and the vesicles. A cluster theory is developed to approximate the exact clustering properties stemming from the simulations. It is shown that the theory is able to reproduce the micellisation phenomenon.

1 Introduction

In the statistical mechanics of fluids [1] the liquid state [2] is a particularly fascinating one. A liquid is neither a gas nor a solid, but the state where correlations really play an important role. The pioneering work of Alder [3] showed that, because of the absence of attractive forces, the hard-sphere fluid admits only a single fluid phase. In order to find the liquid phase it is sufficient to add an attractive square-well to the pair-potential of the hard-spheres. The resulting hard-sphere square-well fluid admits a bell-shaped gas-liquid coexistence curve [4,5] with the critical point moving at low temperatures and high densities as the attractive well width diminishes. Recently Kern and Frenkel [6] studied, through computer experiments, a new fluid model made of hard-spheres with patchy square-well attractions. In its simplest version, the single patch case, the model only depends on the surface coverage χ of the patch and the attraction range. Between the two extreme cases $\chi = 0$, the hard-sphere model, and $\chi = 1$, the hard-sphere square-well model, where the particles pair-potential is isotropic, the particles interaction is directional. The $\chi = 1/2$ model is known as the Janus case, as the particle, like the roman God, has two faces of different functionalities.

Another important process, which may lead to the manifestation of macroscopic phenomena, in certain fluids, is the clustering or association. In 1956, for example, Cooper [7] found that the stable state of the degenerate electron fluid in a metal is one in which particles of opposite spin and opposite momentum form pairs. It was then understood that whereas the electrons in a metal form pairs with relative angular momentum zero, in ^{3}He this would be prevented by the hard core repulsion, and that therefore Cooper pairing had to occur in a state of finite angular momentum. In 1961 Lenard [8] proved analytically that a two-component plasma living in one dimension undergoes a transition from the conducting to the insulating state by the formation of neutral dimers made of a positive and a negative charge. A two-component plasma living in two dimensions is only stable at sufficiently high temperatures [9]. But if one adds a hard core to the charges it remains stable even at low temperatures where it undergoes the same transition [10]. The hard core gives rise to anyonic statistics for the quantum fluid living in two dimensions [11]. In three dimensions the two-component plasma with a hard core, the so called restricted-primitive model, also undergoes the clustering transition at low temperature and low densities [12]. An example of a one-component Janus fluid undergoing association is the dipolar hard-sphere fluid. Here a particle can be viewed as the superposition of two uniformly charged spheres: a positive one and a negative one [13].

In their study of the Kern and Frenkel single patch $\chi = 1/2$ Janus case, Sciortino et al. [14] found that the gas branch of the coexistence curve bends at high densities at low temperatures. Below the critical point, the fluid tends to remain in the gas phase for a larger interval of densities respect to the $\chi = 1$ case. This behaviour is due to the tendency of particles to associate due to the directional attractive component in the pair-potential and form clusters. At low temperatures, these clusters interact weakly amongst themselves because the particles of which they are composed tend to expose the hard-sphere hemisphere on the outside of the collapsed cluster.

By studying the clustering properties of the gas phase of the Janus fluid, Sciortino et al. discovered that below the critical temperature there is a range of temperatures where there is formation of two kinds of preferred clusters: the micelles and the vesicles. In the former the particles

[a] e-mail: rfantoni27@sun.ac.za

tend to arrange themselves into a spherical shell and in the latter they tend to arrange themselves as two concentric spherical shells.

It is important to confront existing cluster theories with these new findings based on computer experiments. In this work the Bjerrum cluster theory for electrolytes, later extended by Tani and Henderson [15] to include trimers, has been employed (preliminary results appeared in Ref. [16]) for the description of the exact equilibrium cluster concentrations found in the computer experiment of Sciortino et al. The theory is extended to clusters of up to 12 particles in an attempt to reproduce the micellisation phenomenon observed in the simulations around a reduced temperature of 0.27. A different determination of the intra-cluster configurational partition function has been devised in place of the one used by Lee et al. [17].

The Kern and Frenkel fluid has been used to describe soft matter [18] biological and non-biological materials like globular proteins in solution [6,19,20] and colloidal suspensions [6,21], or molecular liquids [22]. Recently there has been a tremendous development in the techniques for the synthesis of patchy colloidal particles [23,24] in the laboratory. These are particles with dimensions of 10–10^4 Å in diameter, which obey to Boltzmann statistics[1]. From the realm of patchy colloidal particles stems the family of Janus particles for their simplicity [25,26]. It is possible to create Janus particles in the laboratory in large quantities [27] and to study their clustering properties [28,29].

The micelles and the vesicles are complex structures observed in the chemistry of surfactant molecules analogous to those which may be found in the physical biology of the cell [30].

The paper is organized as follows: in Section 2 we describe the fluid model, in Section 3 we present the clustering properties of the fluid found in the Monte Carlo simulations of Sciortino et al., the cluster theory is presented and developed in Sections 4 and 5, in Section 6 we compare the numerical results from our approximation to the exact results of Sciortino et al., and Section 7 is for final remarks.

2 The Kern and Frenkel model

As in the work of Sciortino et al. [14] we use the Kern and Frenkel [6] single patch hard-sphere model of the Janus fluid. Two spherical particles attract via a square-well potential only if the line joining the centers of the two spheres intercepts the patch on the surfaces of both particles. The pair-potential is separated as follows:

$$\Phi(1,2) = \phi(r_{12})\Psi(\hat{\mathbf{n}}_1, \hat{\mathbf{n}}_2, \hat{\mathbf{r}}_{12}), \tag{1}$$

where

$$\phi(r) = \begin{cases} +\infty & r < \sigma \\ -\epsilon & \sigma < r < \lambda\sigma \\ 0 & \lambda\sigma < r \end{cases} \tag{2}$$

and

$$\Psi(\hat{\mathbf{n}}_1, \hat{\mathbf{n}}_2, \hat{\mathbf{r}}_{12}) = \begin{cases} 1 \text{ if } \hat{\mathbf{n}}_1 \cdot \hat{\mathbf{r}}_{12} \geq \cos\theta_0 \\ \quad \text{and } -\hat{\mathbf{n}}_2 \cdot \hat{\mathbf{r}}_{12} \geq \cos\theta_0 \\ 0 \text{ otherwise} \end{cases} \tag{3}$$

where θ_0 is the angular semi-amplitude of the patch. Here $\hat{\mathbf{n}}_i(\omega_i)$ are versors pointing from the center of sphere i to the center of the attractive patch, with ω_i their solid angles and $\hat{\mathbf{r}}_{12}(\Omega)$ is the versor pointing from the center of sphere 1 to the center of sphere 2, with Ω its solid angle. We denote with σ the hard core diameter and $\lambda = 1+\Delta/\sigma$ with Δ the width of the attractive well.

A particle configuration is determined by its position and its orientation.

We will use σ as the unit of length and ϵ as the unit of energy.

One can determine the fraction of the particle surface covered by the attractive patch as follows

$$\chi = \langle \Psi(\hat{\mathbf{n}}_1, \hat{\mathbf{n}}_2, \hat{\mathbf{r}}_{12}) \rangle^{1/2}_{\omega_1,\omega_2} = \sin^2\left(\frac{\theta_0}{2}\right), \tag{4}$$

where $\langle \ldots \rangle_\omega = \int \ldots d\omega/(4\pi)$.

As in the work of Sciortino et al. [14] we limit ourselves to the Janus case $\chi = 1/2$.

3 Clustering properties

The Janus fluid just described will undergo clustering as there is a directional attractive component in the interaction between its particles. Moreover at low temperatures the collapsed clusters are expected to interact weakly with each other. This is responsible for the bending at high density of the low temperature gas branch of the gas-liquid binodal curve recently determined in reference [14]. Below the critical temperature, in the vapour phase, the appearance of weakly interacting clusters destabilizes the liquid phase in favour of the gas phase. Sciortino et al. during their canonical ensemble (at fixed number of particles N, volume V, and temperature T, with $\rho = N/V$ the density) Monte Carlo simulations of the fluid also studied its clustering properties. In particular they used the following topological definition of a cluster: an ensemble of n particles form a cluster when, starting from one particle, is possible to reach all other particles through a path. The path being allowed to move from one particle to another if there is attraction between the two particles. During the simulation of the fluid they counted the number N_n of clusters of n particles, which depends on the particles configurations, and took a statistical average of this number.

We show in Figure 1 the results they obtained for $\Delta = \sigma/2$ at a reduced density $\rho\sigma^3 = 0.01$ and various reduced

[1] The quantum effects start playing a role when the de Broglie thermal wavelength $\Lambda = \sqrt{2\pi\hbar^2/(k_B T m)}$ becomes comparable to the particle diameter σ. At room temperature this means that the nanoparticles should have a mass of the order of 10^{-26} kg whereas the microparticles should have a mass of the order of 10^{-32} kg.

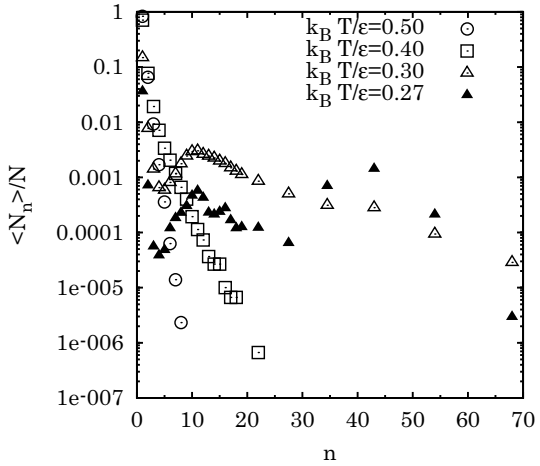

Fig. 1. Exact cluster concentrations of the Janus fluid with $\Delta = \sigma/2$ at a reduced density $\rho\sigma^3 = 0.01$ and various reduced temperatures k_BT/ϵ, from the Monte Carlo simulation of Sciortino et al. [14].

temperatures k_BT/ϵ. From the figure we can see how at a reduced temperature of 0.27, in the vapour phase, there is the formation of two kinds of preferred clusters: one made up of around 10 particles and one made up of around 40 particles.

In their collapsed shape, expected at low temperatures, the particles in the clusters tend to expose their inactive hemisphere on the outside of the cluster, resulting in a weak interaction between pairs of clusters.

In the clusters of around 10 particles the particles tend to arrange themselves into a spherical shell, forming a micellar structure. In the clusters of around 40 particles the particles are arranged into two concentric spherical shells, forming a vesicular structure.

The aim of the present work is to see if we can approximate the exact equilibrium cluster concentrations found in the simulation using a cluster theory. We will restrict ourselves to clusters made of up to 12 particles to see if the theory is able to reproduce the micellisation phenomenon. The theory is described next.

4 A cluster theory for Janus particles

Following reference [15], we describe the fluid of N particles undergoing clustering as a mixture of N species of clusters. Clusters of species $n = 1, \ldots, N$, which we call n-clusters, are made up of n particles. We denote with N_n the number of clusters of species n and with $\rho_n = N_n/V$ their density. We assume that the chemical potentials of all the cluster species are zero (there is no cost in energy in the formation or destruction of a cluster). Then the grand-canonical partition function of the fluid can be written as

$$Q_{\rm tot} = {\sum_{\{N_n\}}}' \prod_{n=1}^{N} \frac{1}{N_n!} \left(q_n^{\rm intra}\right)^{N_n} Q_{\rm inter}\left(\{N_n\}, V, T\right), \quad (5)$$

where one separates the coordinates and momenta relative to the center of mass of a cluster from the ones of the center of mass so that $q_n^{\rm intra}$ will be the intra-cluster partition function of the cluster of species n and $Q_{\rm inter}$ the inter-cluster partition function where we consider the clusters as non identical. The prime indicates that the sum is restricted by the condition that the number of particles of the fluid is N,

$$\sum_{n=1}^{N} nN_n = N. \quad (6)$$

We approximate $Q_{\rm tot}$ assuming that the sum can be replaced by its largest dominant contribution. Using the Stirling approximation $N! \approx (N/e)^N$ one then obtains

$$\ln Q_{\rm tot} \approx \sum_{n=1}^{N} \left[N_n \ln q_n^{\rm intra} - (N_n \ln N_n - N_n)\right] + \ln Q_{\rm inter}. \quad (7)$$

The maximum of $\ln Q_{\rm tot}$ as a function of $\{N_n\}$ on the constraint of equation (6) is given by the point $\{\overline{N}_n\}$ where the gradients of $\ln Q_{\rm tot}$ and of the constraint have the same direction. Introducing a Lagrange multiplier λ the equilibrium cluster distribution $\{\overline{N}_n\}$ is then found from the conditions

$$\frac{\partial}{\partial N_n} \ln Q_{\rm tot}\bigg|_{\{N_n=\overline{N}_n\}} + \ln \lambda^n = 0, \quad n = 1, 2, 3, \ldots \quad (8)$$

The resulting Helmholtz free energy, $\beta F_{\rm tot} = -\ln Q_{\rm tot}$, can then be written in terms of the intra-cluster free energy, $\beta f_n^{\rm intra} = -\ln q_n^{\rm intra}$, and the inter-cluster partition function as follows

$$\frac{\beta F_{\rm tot}}{V} = \sum_{n=1}^{N} \left[\overline{\rho}_n \ln \overline{\rho}_n - \overline{\rho}_n\right] + \sum_{n=1}^{N} \overline{\rho}_n \beta f_n^{\rm intra} + \sum_{n=1}^{N} \overline{\rho}_n \ln V - \frac{1}{V} \ln Q_{\rm inter}, \quad (9)$$

where $\beta = 1/k_BT$ with k_B Boltzmann constant and $\overline{\rho}_n = \overline{N}_n/V$.

We expect the equilibrium cluster concentrations, $\overline{N}_n/N$, to approximate the ones measured in the simulation, $\langle N_n \rangle/N$.

5 Relationship between the configurational partition functions

We will assume that equation (5) also holds at the level of the configurational partition functions Z, as follows

$$Z_{\rm tot} = {\sum_{\{N_n\}}}' \prod_{n=1}^{N} \frac{1}{N_n!} \left(z_n^{\rm intra}\right)^{N_n} Z_{\rm inter}\left(\{N_n\}, V, T\right). \quad (10)$$

In the calculation we only work at the level of the configurational partition functions.

Since we expect the clusters to be weakly interacting amongst themselves we will approximate the inter-clusters configurational partition function with: (i) the ideal gas approximation for pointwise clusters and (ii) the Carnahan-Starling approximation [31] for clusters of diameter σ_0. A third possibility, that we have not investigated, would be to use the Boublík et al. approximation [32,33] for clusters of different diameters σ_n.

We will only work with a limited number n_c of different cluster species. Since we are investigating whether the cluster theory is able to reproduce the micellisation phenomenon we will only consider the first n_c clusters: $n = 1, 2, 3, \ldots, n_c$. And choosing $n_c = 12$.

We will describe next the two approximations used for the inter-cluster configurational partition function.

5.1 Ideal gas approximation

The simplest possibility is to approximate the mixture of clusters as an ideal one so that

$$Z_{\text{inter}} = V^{N_t}, \tag{11}$$

where $N_t = \sum_n N_n$ is the total number of clusters.

The equations for the equilibrium numbers of clusters are

$$\overline{N}_n = \lambda^n V z_n^{\text{intra}}, \quad n = 1, 2, 3, \ldots, n_c \tag{12}$$

$$N = \sum_n n\overline{N}_n, \tag{13}$$

from which we can determine all the concentrations $\overline{N}_n/N$ and the Lagrange multiplier by solving the resulting algebraic equation of order n_c. The case $n_c = 2$ is described in Appendix A.

5.2 Carnahan-Starling approximation

A better approximation is found if we use as the inter-cluster configurational partition function the Carnahan-Starling expression [31] for hard-spheres of diameter σ_0,

$$\ln Z_{\text{inter}} = N_t \ln V - N_t \frac{\eta_t(4 - 3\eta_t)}{(1 - \eta_t)^2}, \tag{14}$$

where $\eta_t = (\pi/6)\rho_t\sigma_0^3$ is the clusters packing fraction and $\rho_t = N_t/V$ their density.

In this case one needs to solve a system of $n_c + 1$ coupled transcendental equations,

$$\overline{N}_n = \lambda^n V z_n^{\text{intra}} G(\overline{\eta}_t), \quad i = 1, 2, 3, \ldots, n_c \tag{15}$$

$$N = \sum_n n\overline{N}_n, \tag{16}$$

with $\overline{\eta}_t = (\pi/6)\overline{\rho}_t\sigma_0^3$, $\overline{\rho}_t = \overline{N}_t/V$, $\overline{N}_t = \sum_n \overline{N}_n$, and

$$G(x) = \exp\left[-\frac{x(8 - 9x + 3x^2)}{(1 - x)^3}\right]. \tag{17}$$

In order to search for the correct root of this system of equations it is important to choose the one that is continuously obtained from the physical solution of the ideal gas approximation as $\sigma_0 \to 0$. Giving a volume to the clusters we introduce correlations between them which will prove to be essential for a qualitative reproduction of the micellisation phenomenon though the cluster theory. The Carnahan-Starling approximation amounts to choosing for the sequence of virial coefficients of the hard-spheres, a general term which is a particular second order polynomial and to determine the polynomial coefficients that approximate the third virial coefficient by its closest integer [31]. It could be interesting to repeat the calculation using for the inter-cluster partition function the hard-spheres one choosing all but the first virial coefficient equal to zero, to see if that is sufficient to reproduce the micellisation phenomena.

Note that in order to study the vesicles we would have to solve a system of around 40 coupled equations.

We will describe next how do we determine the intra-cluster configurational partition function z_n^{intra}.

5.3 The intra-cluster configurational partition function

To estimate the intra-cluster configurational partition function we performed Monte Carlo simulations of an isolated topological cluster.

We determined the reduced excess internal energy per particle of the n-cluster $u_n^{\text{ex}} = \langle \sum_{i<j}^{n} \Phi(i,j) \rangle / (n\epsilon)$ ($u_1^{\text{ex}} = 0$ by definition) as a function of the temperature, and then used thermodynamic integration to determine the intra-cluster configurational partition function.

We found that the results for $u_n^{\text{ex}}(T^\star)$ can be fitted by a Gaussian as follows

$$u_n^{\text{ex}}(T^\star) = a_n e^{-b_n T^{\star 2}} + c_n, \tag{18}$$

with $T^\star = k_B T/\epsilon$ the reduced temperature.

Given the excess free energy of the n-cluster $F_n^{\text{ex,intra}}$, we can then determine $f_n^{\text{ex,intra}} = \beta F_n^{\text{ex,intra}}/n$ as follows

$$\begin{aligned} f_n^{\text{ex,intra}}(\beta^\star) &= \int_0^{\beta^\star} u_n^{\text{ex}}(1/x)\, dx \\ &= c_n\beta^\star + a_n\sqrt{b_n}\left\{\frac{e^{-b_n/\beta^{\star 2}}}{\sqrt{b_n/\beta^{\star 2}}}\right. \\ &\quad \left. + \sqrt{\pi}\left[\operatorname{erf}\left(\sqrt{b_n/\beta^{\star 2}}\right) - 1\right]\right\}, \end{aligned} \tag{19}$$

with $\beta^\star = 1/T^\star$ and $v_0 = \pi\sigma_0^3/6$ the volume of the n-cluster. Then the intra-cluster configurational partition function is given by $z_n^{\text{intra}} = v_0^n \exp(-n f_n^{\text{ex,intra}})$ with $z_1^{\text{intra}} = v_0$.

We studied only the first 10 clusters with $n = 3, \ldots, 12$. The dimer being trivial. To this end we started with an initial configuration of two pentagons with particles at

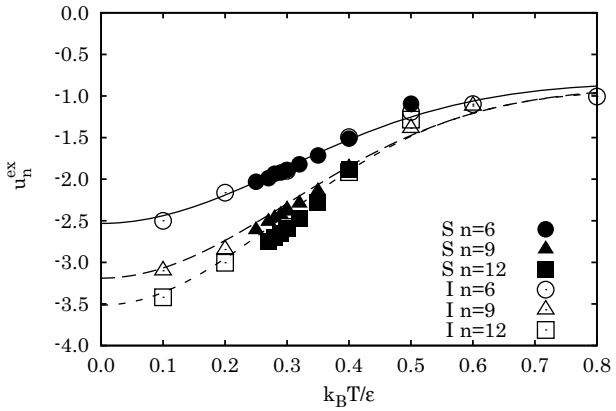

Fig. 2. Reduced excess internal energy per particle as a function of temperature for the 6-, 9-, and 12-cluster. The results from the isolated (I) cluster calculation are compared with the results of Sciortino (S) for the Janus fluid with $\Delta = \sigma/2$ at a reduced density $\rho\sigma^3 = 0.01$. Also shown is the Gaussian fit of equation (18).

their vertexes juxtaposed one above the other. The two pentagons are parallel to the (x, y) plane, have the z axis passing through their centers, and are placed one at $z = +\sigma/2$ and the other at $z = -\sigma/2$. The particles patches all point towards the origin. We formed the clusters with a lower number of particles by simply deleting particles and the clusters with 11 and 12 particles by adding a particle on the z axis just above the upper pentagon and just below the lower one.

We performed the simulations of the isolated cluster at a fictitious reduced density of $\rho\sigma^3 = 0.05$ which ensured a simulation box big enough that the cluster did not percolate through the periodic boundary conditions. We also compared our results for the excess internal energy calculation for the isolated cluster with the results of Sciortino et al. for the low density Janus fluid, from which one extracts cluster information by taking all the clusters found with the same number of particles and averaging their properties, as shown in Figure 2.

At high temperatures the limiting value for the excess internal energy per particle of the isolated n-cluster is $-\epsilon(n-1)/n$ corresponding to the stretched cluster. At low temperature ($T^\star < 0.15$) the cluster tends to freeze into certain energy minima. So in order to reach the absolute minimum we used the following smoothing procedure. We smoothed the Kern and Frenkel potential by choosing

$$\Psi(\hat{\mathbf{n}}_1, \hat{\mathbf{n}}_2, \hat{\mathbf{r}}_{12}) = \{\tanh[l(\hat{\mathbf{n}}_1 \cdot \hat{\mathbf{r}}_{12} - \cos\theta_0)] + 1\} \times \{\tanh[l(-\hat{\mathbf{n}}_2 \cdot \hat{\mathbf{r}}_{12} - \cos\theta_0)] + 1\}/4. \quad (20)$$

We then gradually changed the parameter l, during the simulation, starting from 1/2 and increasing up to values where there is no actual difference between the smoothed potential and the original stepwise one. The reduced excess internal energy per particle and gyration radii for such minimum energy configurations are shown in Table 1.

Table 1. The low temperature reduced excess internal energy per particle $\langle U\rangle/(\epsilon n)$ (U is the potential energy of the cluster) of the clusters with up to 12 particles when $\Delta = \sigma/2$. Also shown is the gyration radius $R_g^2 = \sum_{i=1}^n |\mathbf{r}_i - \mathbf{r}_{cm}|^2/n$ with $\mathbf{r}_{cm} = \sum_{i=1}^n \mathbf{r}_i/n$, $\mathbf{r}_i$ being the position of the ith particle in the cluster.

n	$\langle U\rangle/(\epsilon n)$	$\langle U\rangle/\epsilon$	R_g
1	0	0	0
2	–0.5	–1	$\sim 1/2$
3	–1	–3	$\sim 1/\sqrt{3}$
4	–1.5	–6	0.83
5	–2.0	–10	0.76
6	–2.50	–15	0.75
7	–2.71	–19	0.91
8	–2.88	–23	0.93
9	–3.10	–28	0.96
10	–3.20	–32	1.00
11	–3.36	–37	1.04
12	–3.42	–41	1.08

In the Metropolis algorithm [34] used to sample the probability distribution function proportional to $e^{-\beta U}$, where U is the potential energy of the cluster, the random walk moves through the configuration space of the particles forming the cluster through two kinds of moves: a displacement of the particle position and a rotation of the particle (through the Marsaglia algorithm [35]). We followed two different strategies in the simulations: (i) we averaged only over the particles configurations that form a cluster and (ii) we explicitly modified the acceptance probability by rejecting moves that break the cluster. So in the second strategy all the moves are counted in the averages. The two strategies turned out to give the same results, as they should. The second strategy is preferable to simulate the bigger clusters at high temperature and for small well widths because there is no loss of statistics.

In Appendix B we present the results for the reduced excess internal energy of the isolated clusters as a function of temperature and their fit of equation (18).

5.4 Thermodynamic quantities

Once the equilibrium cluster distribution $\{\overline{N}_n\}$ has been determined (within the ideal gas or the Carnahan-Starling approximation for the inter-cluster partition function) the configurational partition function $Z_{\rm tot}$ is known. Then the excess free energy is

$$\beta F^{\rm ex} = -\ln\left(\frac{Z_{\rm tot}}{V^N}\right), \quad (21)$$

the reduced internal energy per particle of the fluid is

$$u = \frac{3}{2\beta^\star} + \frac{1}{N}\frac{\partial(\beta F^{\rm ex})}{\partial\beta^\star} = \frac{3}{2\beta^\star} - \sum_n \frac{\overline{N}_n}{N}\frac{\partial \ln z_n^{\rm intra}}{\partial\beta^\star} = \frac{3}{2\beta^\star} + \sum_n n\frac{\overline{N}_n}{N}u_n^{\rm ex}, \quad (22)$$

and its compressibility factor, in the Carnahan-Starling approximation for the inter-cluster configurational partition function, is

$$\frac{\beta P}{\rho} = \frac{1}{\rho}\frac{\partial \ln Z_{\rm tot}}{\partial V} \approx \frac{1}{\overline{\rho}_t}\frac{\partial \ln Z_{\rm inter}}{\partial V} = \frac{1+\overline{\eta}_t+\overline{\eta}_t^2-\overline{\eta}_t^3}{(1-\overline{\eta}_t)^3}. \quad (23)$$

Here we have used the approximation $N \approx \overline{N}_t$ which turns out to be reasonable at the chosen value of the cluster diameter, as shown in Figure 4.

In Figure 6 we show the results for the compressibility factor and the reduced excess internal energy per particle. The reduced excess internal energy is compared with the Monte Carlo data of Sciortino et al. (Fig. 1 in Ref. [14]).

6 Results

We present here the numerical results from the cluster theory and compare them with the results of Sciortino et al. from the simulation of the Janus ($\chi = 1/2$) fluid with $\Delta = \sigma/2$.

We studied three different attraction ranges: $\Delta = \sigma/2$, $\Delta = \sigma/4$, and $\Delta = 0.15\sigma$. To the best of our knowledge there are no Monte Carlo results available for the two smaller ranges.

We only present the results obtained from the Carnahan-Starling approximation for the inter-cluster partition function as the ideal gas approximation turned out to be too crude an approximation even for a qualitative description of the exact clustering properties.

6.1 $\Delta = \sigma/2$

For $\Delta = \sigma/2$ we found the following results.

6.1.1 Equilibrium cluster concentrations

In Figure 3 we compare the Monte Carlo data of Sciortino et al. (the results reported in Fig. 1) and our results from the cluster theory. From the figure one can see that the ideal gas approximation for the inter-cluster partition function is not appropriate even at high temperatures in the single fluid phase above the critical point. In order to find agreement with the Monte Carlo data at high temperatures it is sufficient to give a volume to the clusters, treating them as hard-spheres of a diameter σ_0. In the Carnahan-Starling approximation we gradually increased σ_0 from zero and found that for $\sigma_0 = 2.64\sigma$ the results of the cluster theory were in good agreement with the Monte Carlo data at $k_BT/\epsilon = 0.5$. Using the same cluster diameter at all other temperatures, we saw that the theory is able to qualitatively reproduce the micellisation phenomenon observed in the simulation of Sciortino et al.

The results also suggest that with a temperature-dependent cluster diameter, or more generally with a cluster diameter dependent on the thermodynamic state of the

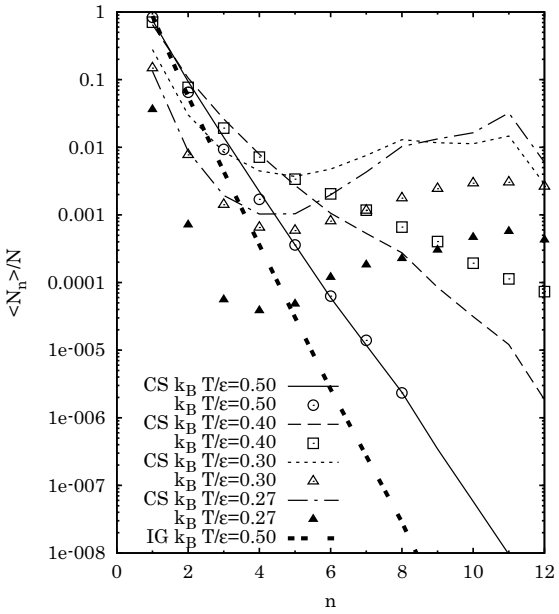

Fig. 3. Comparison between the Monte Carlo (MC) data (points) and the Carnahan-Starling (CS) approximation with $\sigma_0 = 2.64\sigma$ (lines) for the cluster concentrations $\langle N_n\rangle/N$, $n = 1, 2, 3, \ldots, 12$, as a function of the cluster size n at $\rho\sigma^3 = 0.01$ and various temperatures. Also shown is the ideal gas (IG) approximation at the same density and the highest temperature $k_BT/\epsilon = 0.5$.

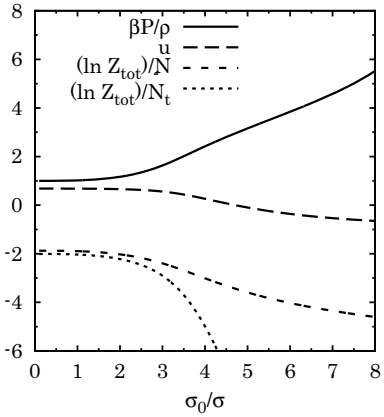

Fig. 4. The compressibility factor, the internal energy per particle, and the logarithm of the total partition function per total number of particles and per total number of clusters as a function of the clusters diameter σ_0 at the thermodynamic state $\rho\sigma^3 = 0.01$ and $k_BT/\epsilon = 0.5$ for $\Delta = 0.5\sigma$.

fluid, we could achieve better agreement between our approximation and the exact results. Our topological definition of a cluster has no direct geometrical interpretation. Other definitions with a geometrical nature are possible. For example Lee et al. in their studies of nucleation define an assembly of particles to be a cluster if they all lie within a sphere of radius σ_0 centered on one of the particles. In our simulations of the isolated clusters these have a globular shape at low temperature and a necklace shape at high temperature. The optimal cluster diameter $\sigma_0 = 2.64\sigma$ (found to give good agreement

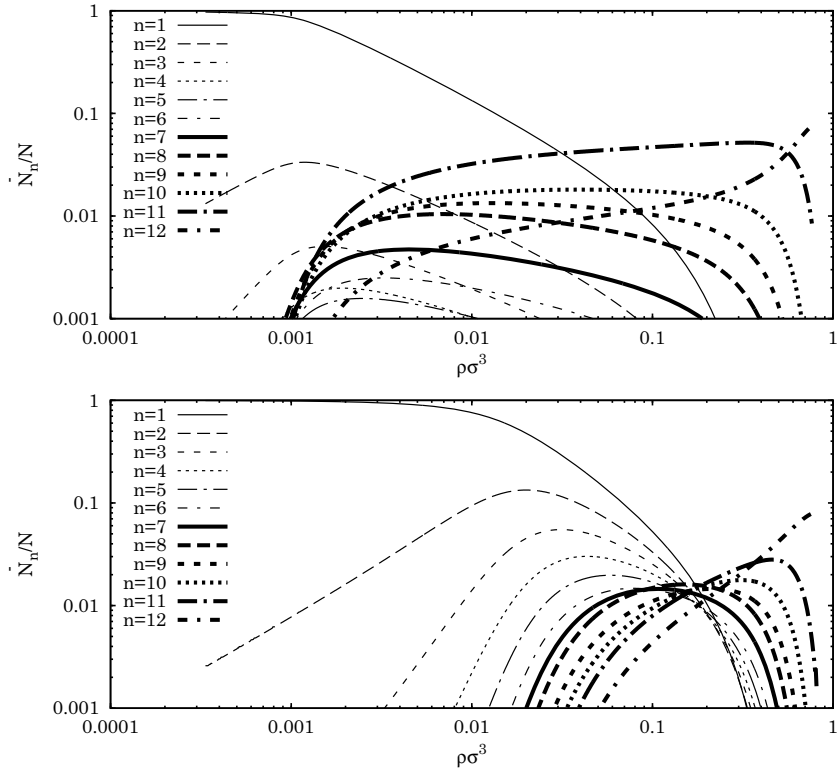

Fig. 5. The equilibrium cluster concentrations $\overline{N}_n/N$, $n = 1, 2, 3, \ldots, 12$, as a function of density for $k_BT/\epsilon = 0.27$ (top panel) and $k_BT/\epsilon = 0.5$ (bottom panel) as obtained from the CS approximation with $\sigma_0 = 2.64\sigma$. Here $\Delta = \sigma/2$.

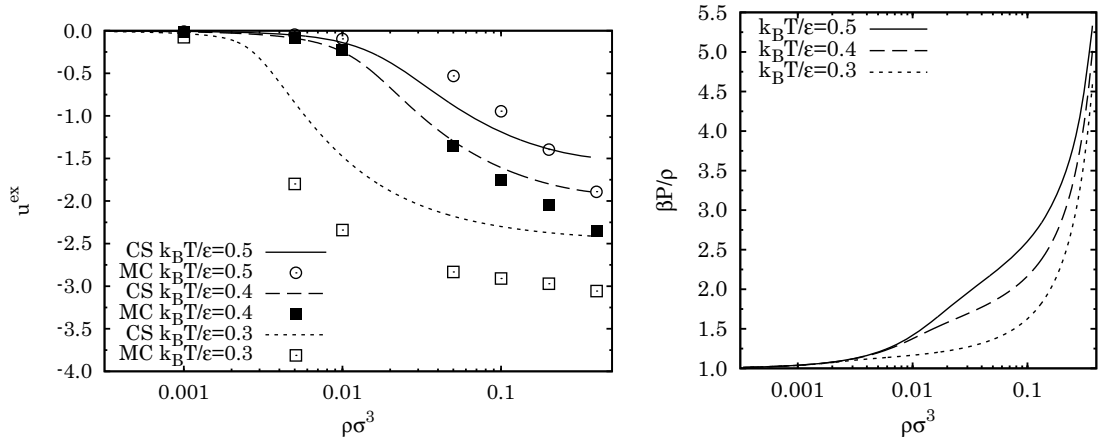

Fig. 6. The top panel shows the reduced excess internal energy per particle for three different values of temperature as a function of density. The results from the Carnahan-Starling (CS) approximation are compared with the Monte Carlo (MC) results of Sciortino et al. [14]. The bottom panel shows the compressibility factor for the same values of temperature as a function of density from the CS approximation (no MC data is available).

between the exact and approximate clusters concentrations at high temperature) suggests necklace clusters made up of around 3 particles or globular clusters made up of around $2\pi(\sigma_0/\sigma)^2/\sqrt{3} \approx 25$ particles placed on a spherical shell. Since σ_0 is the only free parameter of the theory, it is important to estimate how thermodynamic quantities like the compressibility factor $\beta P/\rho$, the reduced internal energy per particle u, and the logarithm of the total configurational partition function per number of particles, $\ln Z_{\rm tot}/N$, or per number of clusters, $\ln Z_{\rm tot}/\overline{N}_t$, are sensible to variations in σ_0. From Figure 4 we can see that for the thermodynamic state $\rho\sigma^3 = 0.01$ and $k_BT/\epsilon = 0.5$, the thermodynamic quantities are roughly independent of σ_0 for $\sigma_0 \lesssim 3\sigma$.

In Figure 5 we show the behaviour of the equilibrium cluster concentrations, from the Carnahan-Starling approximation with $\sigma_0 = 2.64\sigma$, as a function of density at $k_BT/\epsilon = 0.27$.

From the figure we can see that at very low densities there are essentially no clusters. But as the density

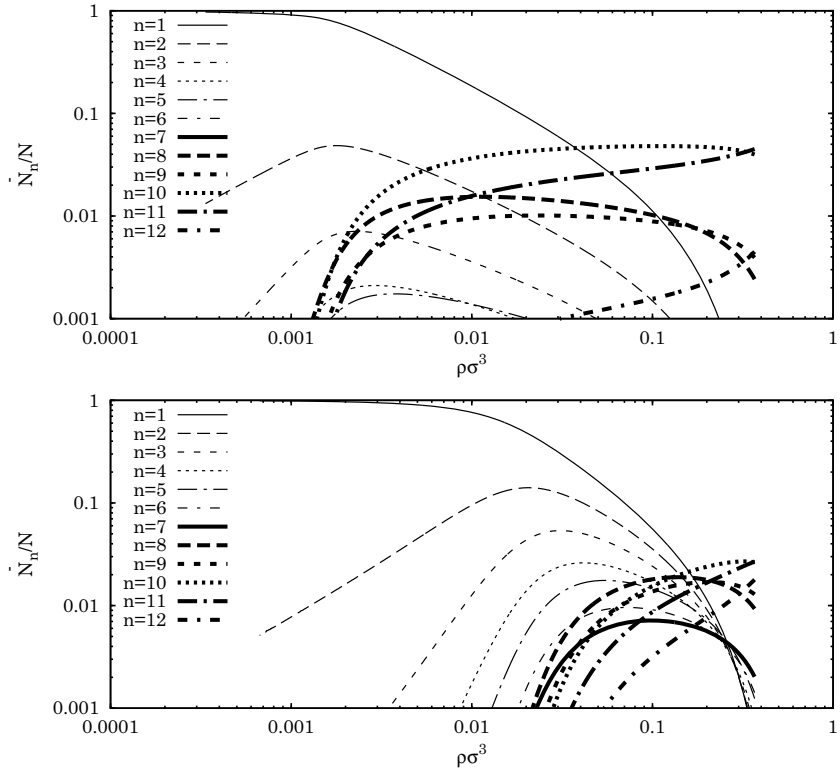

Fig. 7. Same as Figure 5 for $\Delta = \sigma/4$.

increases, clusters of an increasing number of particles appear in the fluid. In particular, at $k_BT/\epsilon = 0.27$ there is an interval of densities where clusters of 11 particles are preferred.

6.1.2 Thermodynamic quantities

Following Section 5.4 we now use the cluster theory within the Carnahan-Starling approximation with $\sigma_0 = 2.64\sigma$ to extract thermodynamic information for the Janus fluid. In Figure 6 we show the results obtained for the excess reduced internal energy per particle and the compressibility factor.

From the figure we see that there is a qualitative agreement between the results of the cluster theory and the Monte Carlo results. No Monte Carlo results are available for the compressibility factor.

6.2 $\Delta = \sigma/4$

Decreasing the width of the attractive well to $\Delta = \sigma/4$ yielded the results shown in Figure 7. We see that now, at the reduced temperature 0.27, the preferred clusters are the ones made up of 10 particles.

6.3 $\Delta = 0.15\sigma$

Decreasing the width of the attractive well even further to $\Delta = 0.15\sigma$, we obtained the results of Figure 8. Now, at the reduced temperature 0.27, there is a range of densities around $\rho\sigma^3 = 0.1$ where the preferred clusters are made up of 7 or 8 particles.

7 Conclusions

We constructed a cluster theory for a fluid undergoing clustering and showed that it is able to reproduce the micellisation phenomena recently observed in the simulation of the vapour phase of Kern and Frenkel Janus particles [14]. A topological definition of the cluster is used. We determined the intra-cluster configurational partition function through thermodynamic integration of the excess internal energy of the cluster, estimated through Monte Carlo simulations of an isolated cluster. In the simulation we restricted the random walk through the configurations of the particles that compose the cluster by rejecting the moves that break the cluster. Due to the geometrical characteristics of the pair-potential it is expected that the clusters, when in their collapsed shape, will be very weakly interacting amongst themselves as the Janus particles will expose the hard-sphere hemisphere on the outside of the cluster. We thus used for the estimation of the inter-cluster configurational partition function first the simple ideal gas approximation for pointwise clusters and then the Carnahan-Starling approximation for clusters seen as hard-spheres of diameter σ_0. The equilibrium cluster concentrations obtained with the ideal gas approximation turned out to disagree, even at high temperatures, with the ones obtained from the simulation of the fluid [14] and were not able to reproduce the micellisation phenomenon in the vapour phase. We then gradually

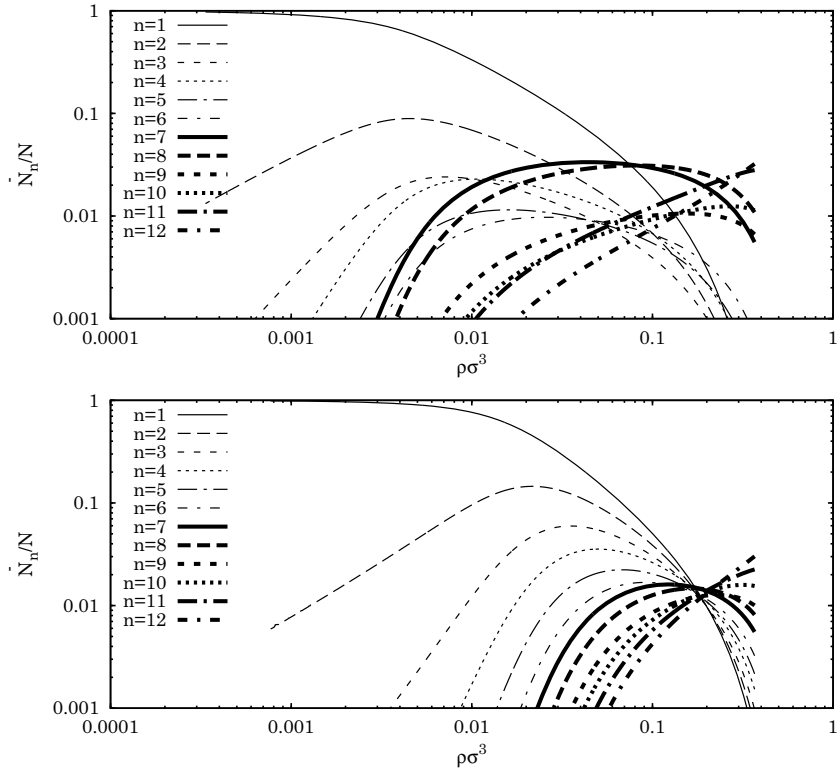

Fig. 8. Same as Figure 5 for $\Delta = 0.15\sigma$.

increased σ_0 from zero until we found good agreement between the equilibrium cluster concentrations obtained with the Carnahan-Starling approximation and the concentrations from the simulation of the fluid [14] at high temperature (above the critical point). Using the same value of σ_0 for lower temperatures (below the critical point) we were able to qualitatively reproduce the micellisation phenomenon observed in the simulation of the fluid [14] around a reduced temperature of 0.27 and a reduced density of 0.01. This result is important for two reasons. Firstly it shows that the clustering fundamentally arising from the canonical ensemble description of the fluid of particles can be approximated by a grand canonical ensemble description of a particular clustered fluid. Secondly the second description, which assumes from the start a clustered structure of the fluid, is much less computationally costly than the first. Unlike most previous works on cluster theories where the aim is usually to avoid the Monte Carlo simulation [15,36], our approach is a hybrid one where we still use the Monte Carlo experiment to determine the intra-cluster properties. Of course our goal can only be a qualitative description of the fluid as we specifically prescribe a particular description of the clusters and this is the source of our approximation.

Studying the behaviour of the equilibrium cluster concentrations as a function of density and temperature, we saw that the micellisation phenomenon only takes place within a particular range of temperatures (below the critical point) and densities (in the vapour phase).

Once the equilibrium concentrations have been found it is possible to determine how the cluster theory approximates the thermodynamic quantities of the fluid. We find qualitative agreement between the Monte Carlo data of Sciortino et al. [14] and our approximation for the excess internal energy of the vapour phase. For the compressibility factor no Monte Carlo data is available so our results remain a theoretical prediction.

We studied three different values of the attractive square-well width: $\Delta = \sigma/2$, $\Delta = \sigma/4$, and $\Delta = 0.15\sigma$. Monte Carlo results [14] are available only for the largest width. Our study shows that as the range of the attraction diminishes the micelles tend to be made up of a smaller number of particles.

A related interesting problem to that just discussed is the one of trying to give a definition of a liquid drop expected to form in the coexistence region as a result of the condensation instability.

I would like to acknowledge the support of the National Institute for Theoretical Physics of South Africa.

Appendix A: Connection with Wertheim association theory

At small χ, allowing only clusters of one (monomers) and two (dimers) particles, we get

$$\overline{N}_1 = \lambda V z_1^{\text{intra}}, \tag{A.1}$$

$$\overline{N}_2 = \lambda^2 V z_2^{\text{intra}}, \tag{A.2}$$

$$N = \overline{N}_1 + 2\overline{N}_2, \tag{A.3}$$

Table B.1. The tables refer from left to right to clusters made up of $n = 3, 4, \ldots, 12$ particles. U is the potential energy of a cluster of n particles. Below $k_BT/\epsilon = 0.1$ the reduced excess internal energy per particle remains roughly constant in all cases: the smoothing procedure described in Section 5.3 was used. The data was obtained with a Monte Carlo simulation over 5 million steps where one step consists of n particles moves. The strategy (i) described in Section 5.3 was used in the simulations.

k_BT/ϵ	$\langle U\rangle/(\epsilon n)$	Error
∞	–0.666	0
0.8	–0.724	0.001
0.6	–0.747	0.001
0.5	–0.769	0.002
0.4	–0.807	0.001
0.3	–0.877	0.001
0.2	–0.9663	0.0008
0.1	–1	≈0

k_BT/ϵ	$\langle U\rangle/(\epsilon n)$	Error
∞	–0.75	0
0.8	–0.849	0.004
0.6	–0.898	0.004
0.5	–0.961	0.005
0.4	–1.081	0.004
0.3	–1.278	0.003
0.2	–1.460	0.002
0.1	–1.5	≈0

k_BT/ϵ	$\langle U\rangle/(\epsilon n)$	Error
∞	–0.8	0
0.8	–0.942	0.009
0.6	–0.995	0.008
0.5	–1.085	0.008
0.4	–1.322	0.007
0.3	–1.606	0.004
0.2	–1.792	0.003
0.1	–2.0	≈0

k_BT/ϵ	$\langle U\rangle/(\epsilon n)$	Error
∞	–0.833	0
0.8	–1.01	0.03
0.6	–1.10	0.02
0.5	–1.19	0.01
0.4	–1.49	0.01
0.3	–1.899	0.009
0.2	–2.16	0.01
0.1	–2.5	0

k_BT/ϵ	$\langle U\rangle/(\epsilon n)$	Error
∞	–0.857	0
0.8	–1.04	0.04
0.6	–1.12	0.02
0.5	–1.28	0.02
0.4	–1.68	0.02
0.3	–2.11	0.04
0.2	–2.39	0.03
0.1	–2.7	≈0

k_BT/ϵ	$\langle U\rangle/(\epsilon n)$	Error
∞	–0.875	0
0.8	–1.06	0.05
0.6	–1.25	0.05
0.5	–1.27	0.02
0.4	–1.82	0.02
0.3	–2.26	0.01
0.2	–2.60	0.02
0.1	–2.9	≈0

k_BT/ϵ	$\langle U\rangle/(\epsilon n)$	Error
∞	–0.888	0
0.8	–	–
0.6	–1.12	0.03
0.5	–1.39	0.03
0.4	–1.87	0.02
0.3	–2.38	0.01
0.2	–2.85	0.02
0.1	–3.1	≈0

k_BT/ϵ	$\langle U\rangle/(\epsilon n)$	Error
∞	–0.9	0
0.8	–	–
0.6	–	–
0.5	–1.36	0.04
0.4	–1.88	0.02
0.3	–2.46	0.02
0.2	–2.94	0.03
0.1	–3.2	≈0

k_BT/ϵ	$\langle U\rangle/(\epsilon n)$	Error
∞	–0.909	0
0.8	–	–
0.6	–	–
0.5	–1.35	0.03
0.4	–1.96	0.03
0.3	–2.55	0.02
0.2	–3.09	0.09
0.1	–3.36	≈0

k_BT/ϵ	$\langle U\rangle/(\epsilon n)$	Error
∞	–0.916	0
0.8	–	–
0.6	–	–
0.5	–1.28	0.04
0.4	–1.92	0.04
0.3	–2.57	0.02
0.2	–3.00	0.02
0.1	–3.42	≈0

which is a quadratic equation in λ. The solution for the fraction of patches that are not bonded (fraction of monomers) is

$$\frac{\overline{\rho}_1}{\rho} = \frac{2}{1+\sqrt{1+8\rho\overline{\Delta}}}, \tag{A.4}$$

with $\overline{\Delta} = z_2^{\text{intra}}/[z_1^{\text{intra}}]^2$ and $\rho = N/V$ the density of the fluid, in accord, at low T, with the recent analysis of Sciortino et al. [37] (compare their X of Eq. (10) with our $\overline{\rho}_1/\rho$ and their Δ with our $\overline{\Delta}$), based on Wertheim association theory [38–41]. Our theory, contrary to the one of Wertheim, allows to consider the case of multiple bonding of the patch.

At high temperature our $\overline{\Delta}$ differs from the Δ of reference [37] but in this limit the clusters begin to dissociate.

Appendix B: Tables for the excess internal energy per particle of the clusters

We present here the results for the reduced excess internal energy per particle as a function of temperature of the isolated n-cluster with $n = 2, 3, \ldots, 12$ as obtained from our Monte Carlo simulations.

In Table B.1 we show the results at $\Delta = 0.5\sigma$ obtained with the strategy (i) described in Section 5.3. The smoothing procedure described in Section 5.3 was used at the lowest temperature. The excess internal energy per particle of the $n = 2$ cluster is always $-\epsilon/2$ given our topological definition of a cluster.

In Table B.2 we show the results at $\Delta = 0.5\sigma$ obtained with strategy (ii) described in Section 5.3. The smoothing procedure described in Section 5.3 was not used at the lowest temperature. Comparing Tables B.1 and B.2 we can see that the two strategies lead to the same results.

In Table B.3 we show the results at $\Delta = 0.25\sigma$ obtained with strategy (i) described in Section 5.3. The smoothing procedure described in Section 5.3 was not used at the lowest temperature.

In Table B.4 we show the results at $\Delta = 0.15\sigma$ obtained with strategy (ii) described in Section 5.3. The smoothing procedure described in Section 5.3 was not used at the lowest temperature.

In Table B.5 we give the fit to the Gaussian of equation (18) of the reduced excess internal energy per particle as a function of the temperature.

Table B.2. The tables refer, from left to right, to clusters made up of $n = 3, 4, 10, 11$ particles. U is the potential energy of a cluster of n particles. The smoothing procedure described in Section 5.3 was not used at the lowest temperature. The strategy (ii) described in Section 5.3 was used in the simulations.

k_BT/ϵ	$\langle U\rangle/(\epsilon n)$	Error
∞	–0.666	0
0.8	–0.7211	0.0002
0.6	–0.7437	0.0003
0.5	–0.7659	0.0004
0.4	–0.8052	0.0005
0.3	–0.8723	0.0007
0.2	–0.9647	0.0005
0.1	–0.99881	0.00005

k_BT/ϵ	$\langle U\rangle/(\epsilon n)$	Error
∞	–0.75	0
0.8	–0.8466	0.0005
0.6	–0.8995	0.0009
0.5	–0.959	0.001
0.4	–1.073	0.002
0.3	–1.280	0.002
0.2	–1.4597	0.0009
0.1	–1.49871	0.00006

k_BT/ϵ	$\langle U\rangle/(\epsilon n)$	Error
∞	–0.9	0
0.8	–1.066	0.001
0.6	–1.200	0.003
0.5	–1.418	0.009
0.4	–1.884	0.009
0.3	–2.46	0.01
0.2	–2.96	0.03
0.1	–3.1982	0.0006

k_BT/ϵ	$\langle U\rangle/(\epsilon n)$	Error
∞	–0.909	0
0.8	–1.078	0.002
0.6	–1.215	0.003
0.5	–1.423	0.008
0.4	–1.90	0.01
0.3	–2.52	0.02
0.2	–3.13	0.04
0.1	–3.16	0.01

Table B.3. Same as Table B.1 but with $\Delta = 0.25\sigma$. The smoothing procedure described in Section 5.3 was not used at the lowest temperature.

k_BT/ϵ	$\langle U\rangle/(\epsilon n)$	Error
∞	–0.666	0
0.7	–0.705	0.002
0.5	–0.732	0.002
0.3	–0.832	0.002
0.1	–0.99872	0.00008

k_BT/ϵ	$\langle U\rangle/(\epsilon n)$	Error
∞	–0.75	0
0.7	–	–
0.5	–0.866	0.007
0.3	–1.138	0.005
0.1	–1.4987	0.0002

k_BT/ϵ	$\langle U\rangle/(\epsilon n)$	Error
∞	–0.8	0
0.7	–0.87	0.02
0.5	–1.00	0.03
0.3	–1.427	0.008
0.1	–1.7984	0.0002

k_BT/ϵ	$\langle U\rangle/(\epsilon n)$	Error
∞	–0.833	0
0.7	–	–
0.5	–0.95	0.01
0.3	–1.63	0.01
0.1	–2.1656	0.0002

k_BT/ϵ	$\langle U\rangle/(\epsilon n)$	Error
∞	–0.857	0
0.7	–	–
0.5	–0.95	0.01
0.3	–1.79	0.01
0.1	–2.22	0.02

k_BT/ϵ	$\langle U\rangle/(\epsilon n)$	Error
∞	–0.875	0
0.7	–	–
0.5	–	–
0.3	–1.91	0.03
0.1	–2.3706	0.0009

k_BT/ϵ	$\langle U\rangle/(\epsilon n)$	Error
∞	–0.888	0
0.7	–	–
0.5	–	–
0.3	–1.95	0.02
0.1	–2.4416	0.0005

k_BT/ϵ	$\langle U\rangle/(\epsilon n)$	Error
∞	–0.9	0
0.7	–	–
0.5	–	–
0.3	–2.07	0.04
0.1	–2.5969	0.0006

k_BT/ϵ	$\langle U\rangle/(\epsilon n)$	Error
∞	–0.909	0
0.7	–	–
0.5	–	–
0.3	–2.10	0.04
0.1	–2.721	0.002

k_BT/ϵ	$\langle U\rangle/(\epsilon n)$	Error
∞	–0.916	0
0.7	–	–
0.5	–	–
0.3	–2.01	0.03
0.1	–2.730	0.008

Table B.4. Same as Table B.1 but with $\Delta = 0.15\sigma$. The smoothing procedure described in Section 5.3 was not used at the lowest temperature. The strategy (ii) described in Section 5.3 was used in the simulation.

k_BT/ϵ	$\langle U\rangle/(\epsilon n)$	Error
∞	–0.666	0
0.7	–0.6914	0.0003
0.5	–0.7114	0.0004
0.3	–0.792	0.001
0.1	–0.9987	0.0002

k_BT/ϵ	$\langle U\rangle/(\epsilon n)$	Error
∞	–0.75	0
0.7	–0.7903	0.0007
0.5	–0.826	0.002
0.3	–1.138	0.005
0.1	–1.49871	0.00006

k_BT/ϵ	$\langle U\rangle/(\epsilon n)$	Error
∞	–0.8	0
0.7	–0.8473	0.0009
0.5	–0.895	0.002
0.3	–1.230	0.008
0.1	–1.7989	0.0001

k_BT/ϵ	$\langle U\rangle/(\epsilon n)$	Error
∞	–0.833	0
0.7	–0.884	0.001
0.5	–0.936	0.002
0.3	–1.35	0.01
0.1	–1.9985	0.0004

k_BT/ϵ	$\langle U\rangle/(\epsilon n)$	Error
∞	–0.857	0
0.7	–0.913	0.001
0.5	–0.955	0.002
0.3	–1.61	0.03
0.1	–2.2848	0.0001

k_BT/ϵ	$\langle U\rangle/(\epsilon n)$	Error
∞	–0.875	0
0.7	–0.928	0.001
0.5	–0.980	0.003
0.3	–1.63	0.03
0.1	–2.371	0.001

k_BT/ϵ	$\langle U\rangle/(\epsilon n)$	Error
∞	–0.888	0
0.7	–0.945	0.001
0.5	–1.000	0.003
0.3	–1.55	0.06
0.1	–2.51	0.04

k_BT/ϵ	$\langle U\rangle/(\epsilon n)$	Error
∞	–0.9	0
0.7	–0.956	0.001
0.5	–1.013	0.004
0.3	–1.56	0.05
0.1	–2.396	0.001

k_BT/ϵ	$\langle U\rangle/(\epsilon n)$	Error
∞	–0.909	0
0.7	–0.9655	0.0009
0.5	–1.022	0.004
0.3	–1.61	0.03
0.1	–2.5427	0.0004

k_BT/ϵ	$\langle U\rangle/(\epsilon n)$	Error
∞	–0.916	0
0.7	–0.973	0.001
0.5	–1.033	0.002
0.3	–1.59	0.02
0.1	–2.66	0.004

Table B.5. Fit to the Gaussian of equation (18) of the reduced excess internal energy per particle of the first eleven n-clusters as a function of temperature.

	$\Delta = 0.5\sigma$		$\Delta = 0.25\sigma$		$\Delta = 0.15\sigma$		
n	a_n	b_n	a_n	b_n	a_n	b_n	$c_n = -(n-1)/n$
2	0	1	0	1	0	1	–0.5
3	–0.337525	3.88039	–0.33890	6.9050	–0.345587	10.7799	–0.66666
4	–0.778556	4.66976	–0.77059	7.5017	–0.773523	7.97531	–0.75
5	–1.22587	5.16189	–1.0248	5.8901	–1.03428	9.36621	–0.8
6	–1.69844	5.59919	–1.3810	7.3613	–1.20676	9.21365	–0.83333
7	–1.89814	5.26287	–1.4235	6.7666	–1.47964	8.27638	–0.85714
8	–2.06452	5.07916	–1.5201	4.1792	–1.55091	8.50313	–0.875
9	–2.30070	5.47737	–1.5793	4.3672	–1.68144	10.1592	–0.88888
10	–2.39363	5.50909	–1.7253	4.2708	–1.55096	9.41914	–0.9
11	–2.55636	5.64409	–1.8464	4.8294	–1.69591	9.75528	–0.90909
12	–2.59747	6.07744	–1.8541	5.7234	–1.81374	10.5661	–0.91666

References

1. T.L. Hill, *Statistical Mechanics* (McGraw-Hill, New York, 1956)
2. J.-P. Hansen, I.R. McDonald, *Theory of simple liquids*, 3rd edn. (Elsevier, USA, 2006)
3. B.J. Alder, T.E. Wainwright, J. Chem. Phys. **27**, 1208 (1957)
4. L. Vega, E. de Miguel, L.F. Rull, G. Jackson, I.A. McLure, J. Chem. Phys. **96**, 2296 (1992)
5. H. Liu, S. Garde, S. Kumar, J. Chem. Phys. **123**, 174505 (2005)
6. N. Kern, D. Frenkel, J. Chem. Phys. **118**, 9882 (2003)
7. L.N. Cooper, Phys. Rev. **104**, 1189 (1956)
8. A. Lenard, J. Math. Phys. **2**, 682 (1961)
9. E.H. Hauge, P.C. Hemmer, Physica Norvegica **5**, 209 (1971)
10. J.M. Kosterlitz, D.J. Thouless, J. Phys. C Solid State Phys. **6**, 1181 (1973)
11. A. Lerda, *Anyons* (Springer-Verlag, New York, 1992)
12. C. Valeriani, P.J. Camp, J.W. Zwanikken, R. Van Roij, M. Dijkstra, J. Phys.: Condens. Matter **22**, 104122 (2010)
13. L. Rovigatti, J. Russo, F. Sciortino, Phys. Rev. Lett. **107**, 237801 (2011)
14. F. Sciortino, A. Giacometti, G. Pastore, Phys. Rev. Lett. **103**, 237801 (2009)
15. A. Tani, D. Henderson, J. Chem. Phys. **79**, 2390 (1983)
16. R. Fantoni, A. Giacometti, F. Sciortino, G. Pastore, Soft Matt. **7**, 2419 (2011)
17. J.K. Lee, J.A. Barker, F.F. Abraham, J. Chem. Phys. **58**, 3166 (1973)
18. P.G. de Gennes, Rev. Mod. Phys. **64**, 645 (1992)
19. A. Giacometti, F. Lado, J. Largo, G. Pastore, F. Sciortino, J. Chem. Phys. **132**, 174110 (2010)
20. F. Romano, E. Sanz, F. Sciortino, J. Chem. Phys. **132**, 184501 (2010)
21. F. Romano, F. Sciortino, Soft Matt. **7**, 5799 (2011)
22. F. Romano, E. Sanz, F. Sciortino, J. Chem. Phys. **134**, 174502 (2011)
23. S.C. Glotzer, M.J. Solomon, Nature Mater. **6**, 557 (2007)
24. A.B. Pawar, I. Kretzchmar, Macromol. Rapid Comm. **31**, 150 (2010)
25. C. Casagrande, P. Fabre, M. Veyssié, E. Raphaël, Europhys. Lett. **9**, 251 (1989)
26. A. Walther, A.H. Müller, Soft Matt. **4**, 663 (2008)
27. L. Hong, S. Jiang, S. Granick, Langmuir **22**, 9495 (2006)
28. L. Hong, A. Cacciuto, E. Luijten, S. Granick, Nano Lett. **6**, 2510 (2006)
29. L. Hong, A. Cacciuto, E. Luijten, S. Granick, Langmuir **24**, 621 (2008)
30. R. Phillips, J. Kondev, J. Theriot, *Physical Biology of the Cell* (Gerland Science, Taylor & Francis Group, 2008), Problem 9.4
31. N.F. Carnahan, K.E. Starling, J. Chem. Phys. **51**, 635 (1969)
32. T. Boublík, J. Chem. Phys. **53**, 471 (1970)
33. G.A. Mansoori, N.F. Carnahan, K.E. Starling, T.W. Leland Jr., J. Chem. Phys. **54**, 1523 (1971)
34. M.H. Kalos, P.A. Whitlock, *Monte Carlo Methods* (Wiley-VCH Verlag GmbH & Co., Germany, 2008)
35. M.P. Allen, D.J. Tildesley, *Computer Simulation of Liquids* (Oxford University Press, 1987), Appendix G.4
36. J.-M. Caillol, J.-J. Weis, J. Chem. Phys. **102**, 7610 (1995), and references therein
37. F. Sciortino, E. Bianchi, J.F. Douglas, P. Tartaglia, J. Chem. Phys. **126**, 194903 (2007)
38. M.S. Wertheim, J. Stat. Phys. **35**, 19 (1984)
39. M.S. Wertheim, J. Stat. Phys. **35**, 35 (1984)
40. M.S. Wertheim, J. Stat. Phys. **42**, 459 (1986)
41. M.S. Wertheim, J. Stat. Phys. **42**, 477 (1986)